

Duawlfín: A Drone with Unified Actuation for Wheeled Locomotion and Flight Operation

Jerry Tang, Ruiqi Zhang, Kaan Beyduz, Yiwei Jiang, Cody Wiebe, Haoyu Zhang, Osaruese Asoro, and Mark W. Mueller

Abstract—This paper presents Duawlfín, a drone with unified actuation for wheeled locomotion and flight operation that achieves efficient, bidirectional ground mobility. Unlike existing hybrid designs, Duawlfín eliminates the need for additional actuators or propeller-driven ground propulsion by leveraging only its standard quadrotor motors and introducing a differential drivetrain with one-way bearings. This innovation simplifies the mechanical system, significantly reduces energy usage, and prevents the disturbance caused by propellers spinning near the ground, such as dust interference with sensors. Besides, the one-way bearings minimize the power transfer from motors to propellers in the ground mode, which enables the vehicle to operate safely near humans. We provide a detailed mechanical design, present control strategies for rapid and smooth mode transitions, and validate the concept through extensive experimental testing. Flight-mode tests confirm stable aerial performance comparable to conventional quadcopters. And the ground-mode experiments demonstrate efficient slope climbing and agile turning maneuvers. The seamless transitions between aerial and ground modes further underscore the practicality and effectiveness of our approach for applications like urban logistics and indoor navigation. All the materials including 3D model files, demonstration video and other assets are open-sourced at <https://sites.google.com/view/Duawlfín>.

Index Terms—Aerial Systems; mechanics and control; mechanism design; motion control

I. INTRODUCTION

UNCREWED Aerial Vehicles (UAVs) exhibit notable advantages in terms of mobility and terrain adaptability. Due to their ability to operate in three-dimensional space [1], [2], UAVs possess superior maneuverability that can traverse complex or unstructured environments such as rugged terrain, dense vegetation, or urban obstacles without the constraints imposed by ground contact. Such mobility makes UAVs especially suitable for tasks that require rapid deployment, flexible routing and access to otherwise inaccessible locations, like delivery, remote sensing, and infrastructure inspection and monitoring [3]–[5]. However, UAVs also suffer from several intrinsic limitations, which primarily stem from the aerodynamic and propulsion requirements associated with sustained flight. For instance, multirotor UAVs must constantly generate lift equal to their weight through high-speed rotation of propellers, resulting in significant energy expenditure even when hovering [6]. Ground mobility can alleviate some of these issues. By letting aerial robots roll or drive when airborne travel is not essential, energy consumption can be substantially reduced and safety hazards near the ground can be minimized [3]. However,

The authors are with High Performance Robotics Lab, Department of Mechanical Engineering, University of California, Berkeley, CA 94720, United States. (email: richzhang@berkeley.edu, mwm@berkeley.edu)



Fig. 1. Top: Duawlfín is in aerial mode. Bottom: Duawlfín is running on the sidewalk in ground mode. The propellers are still turning at low speed since the friction in the one-way bearings’ free mode.

achieving this aerial–ground versatility is non-trivial. Hybrid robots must incorporate additional hardware or specialized transmissions to enable terrestrial motion, typically adding weight, complexity, and potential failure points [7]–[9]. The goal, then, is to design a hybrid configuration, which can preserve the UAV’s agility and compactness while gaining the energy and functional benefits of ground locomotion.

A. Literature Review

Numerous hybrid aerial–ground vehicles have been proposed to strike a balance between flight capabilities and terrestrial efficiency. Existing designs can be broadly divided into two primary approaches based on how they achieve ground propulsion.

1) *Propeller-driven ground propulsion*: These UAV designs employ angled or redirected thrust from their existing propellers to achieve ground locomotion. Quadroller is a quadrotor with low-friction wheels and skateboard steering trucks that rolls farther than it hovers despite a small mass penalty [10]. In similar fashion, Quadrolltor is a passively reconfigurable quadrotor with a rolling cage that enables controlled turning and improves low-speed ground endurance [11].

Another design named Rollocopter raises a spherical-shell platform that rolls on extreme terrain and flies, balancing power via an energy-aware controller [12]. People also retrofit a quadcopter’s propellers for ground motion and obstacle avoidance without extra actuators [13]. The designers of Delta propose a deformable multirotor that rolls with its entire body and seamlessly switches modes [9]. Similarly, Hopcopter is a quadcopter with a passive leg enabling jumps and efficient ground-to-air transitions [14]. Other researchers design a platform named Skywalker with an omnidirectional wheel and differential-flatness control to achieve up to a speed of 5 m/s and 75.2% energy savings on the ground [15]. A design of terrestrial-aerial bimodal vehicle utilizes nonlinear model predictive control (MPC) with maximum 3 m/s ground velocity [16]. Similarly, Skater is a bi-copter with passive wheels that leverages vectored thrust and MPC for robust terrain traversal and steering [17]. Another bi-copter vehicle integrates a single passive wheel at a UAV’s base, saving 77% battery during rolling [8]. In the latest work, a hybrid quadrotor with a passively reconfigurable wheeled leg can achieve robust ground mobility and turning, while retaining aerial capability [18]. Such an approach offers simplicity, as no additional actuators or motors are required. However, using propellers for ground propulsion generally requires higher power than dedicated wheel actuation, particularly during sustained or high-force maneuvers. Continuous spinning of propellers near the ground may also stir up dust and debris, potentially interfering with onboard sensors and affecting other system components. Additionally, prolonged ground operation can increase thermal loads on motors, possibly reducing their service life [19], and the spinning propellers pose inherent safety concerns.

2) *Additional actuators for ground motion:* The second category equips the robot with dedicated actuators, usually motors driving wheels or legs. As a representative, Drivocopter uses four actuated spherical wheels for long-endurance hybrid mobility and propeller protection [7]. Researchers develop a compact hybrid that transforms between ground and air modes, shielding flight hardware when grounded [20]. SP-IDAR is a quadruped with distributed vectorable rotors for both walking and flight [21]. Similarly, a humanoid with wheels and a flight unit named FlyHuman enables aerial, legged, and wheeled locomotion under unified control [22]. The bipedal platform LEONARDO combines thrusters and multi-joint legs to perform maneuvers such as slackline balancing and skateboarding [23]. MTMUR is an amphibious robot using custom wheels and floats to navigate land, water, and air [24]. M4 designers purpose appendages into wheels, thrusters, and legs for eight distinct locomotion modes [25]. Similarly, other researchers design a robot with avian-inspired legs for walking, hopping, and jump-into-flight transitions which demonstrates improved efficiency over pure propeller takeoff [26]. The advantage of this design lies in the use of two independent sets of actuators, which eliminates concerns about motor overload and allows each actuator to operate efficiently. Moreover, by decoupling the power sources for ground and aerial locomotion, the propellers are not engaged during ground movement, which enhances operational safety. These

designs typically demonstrate robust ground maneuverability but at the expense of higher total mass which in turn reduced flight times. The greater complexity also increases cost and maintenance requirements.

B. Contribution

Despite the diversity of existing hybrid platforms, current designs typically rely either on propeller-driven rolling or on additional terrestrial actuators to enable ground mobility. The field thus remains open to exploring simpler and lighter solutions capable of bidirectional ground travel by leveraging only existing aerial motors, thereby minimizing mechanical complexity and energy use. This paper introduces Duawlfín, a drone with unified actuation for wheeled locomotion and flight operation that achieves efficient, bidirectional ground mobility. Specifically, the contributions of this letter are:

- The proposed hybrid design achieves bidirectional ground mobility using the drone’s *existing* motors only, requires no additional actuators and avoids propeller-based ground propulsion and safety hazard.
- The proposed system integrates a lightweight drivetrain that enables efficient ground driving with only trivial energy loss during flight, supports seamless transitions between modes with no reconfiguration, and allows differential motor control for intuitive bidirectional steering on the ground.
- Comprehensive real-world experiments demonstrate agile but stable flight, ground locomotion with strong slope climbing capability, and fast aerial-ground transitions.

The remainder of this paper is organized as follows: Section II provides a detailed description of the mechanical design of the hybrid robot, highlighting key structural features and the principles enabling dual-mode locomotion. Section III elaborates on the mode-switching control algorithm developed for hybrid mobility. Section IV presents a comprehensive set of real-world experiments, analyses, and evaluations of the system. Finally, Section V concludes the paper and discusses directions for future research.

II. DESIGN

The goal of this work is to develop a hybrid aerial-ground robot capable of both flying and driving using a single unified actuation system. To minimize hardware complexity and weight, the design reuses the drone’s existing motors for both flight and ground propulsion. A key requirement is to ensure that during ground operation, the propellers do not engage or consume energy, thereby avoiding unnecessary aerodynamic drag and power loss. All added components must be as lightweight and as compact as possible.

A. Key Insights

Multirotor UAVs typically employ brushless DC motors, which are electrically capable of bidirectional operation but mechanically constrained due to the aerodynamic design of their propellers. Propellers are usually optimized for thrust

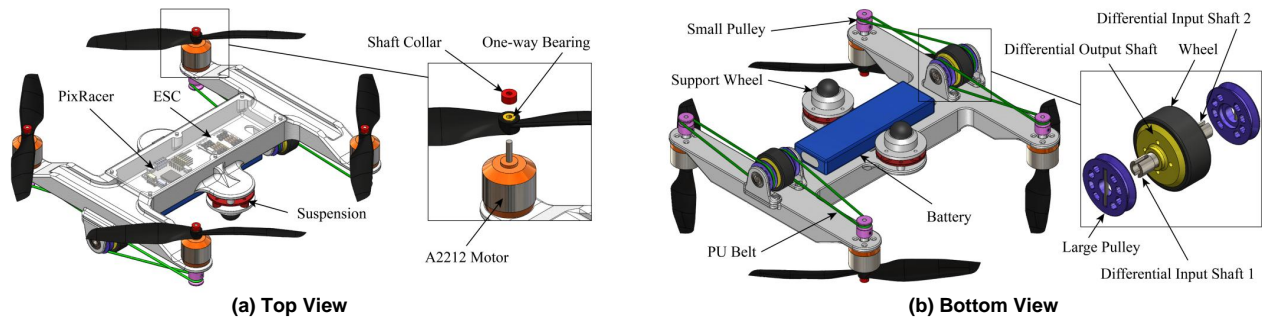


Fig. 2. (a): Top-side view of Duawlfm. It shows its aerial propulsion system. The vehicle features four A2212 1400 KV motors driving 8-inch double-blade (8045-2) propellers. Each propeller is mounted via a one-way bearing and secured by a shaft collar, ensuring that in flight mode the bearings lock to generate thrust, while in ground mode the propellers freewheel. (b): Bottom-side view. It shows the ground drivetrain arrangement. Each motor shaft is equipped with a small pulley that drives a belt connected to a larger pulley on one of the differential's input shafts. Two opposing motors feed their respective differentials, whose output shafts are directly connected to integrated wheels. Universal ball casters at the front and rear provide stable ground support.

generation in only one direction, making reverse rotation highly inefficient in terms of thrust-to-power ratio.

This inherent directional asymmetry can be leveraged for passive mechanical decoupling. By mounting each propeller to its shaft through a one-way bearing, it becomes possible to engage the propeller only during forward motor rotation, which is the optimal direction for aerodynamic thrust, while allowing the propeller to disengage and freely rotate if the motor reverses direction. In such a configuration, reverse motor rotation could potentially be exploited to mechanically harvest torque without unnecessarily spinning the propellers, thus enabling efficient power transfer to a ground drivetrain.

Because motors would spin exclusively in reverse during ground mode, directly coupling each motor to a wheel could lead to unidirectional wheel rotation, severely limiting ground mobility. A differential mechanism, commonly used in automotive applications, can resolve this limitation by combining inputs from two opposing motors. By coupling these motors through pulleys to a central differential, wheel rotation becomes dependent on the relative motor speeds rather than absolute speeds. Equal speeds can yield stationary wheels, while slight speed variations between motors allow wheels to rotate either forward or backward, providing full bidirectional ground mobility. A schematic of the proposed architecture is shown in Fig. 3.

Furthermore, most drone motors are sensorless brushless DC types due to their simplicity and cost efficiency, but this inherently leads to poor startup behavior at very low speeds. A differential mechanism can alleviate this problem by enabling both motors to run at a nominal idle speed during ground operation. In this scenario, as long as motor speeds remain matched, the wheel does not rotate, effectively bypassing the problematic motor startup region. Adjusting relative motor speeds slightly from this nominal point can then produce smooth and controlled wheel motion, improving ground-mode drivability without the need for additional actuators or complex mechanical switching.

B. Experimental Vehicle Design

The hybrid UAV prototype was developed as a custom quadrotor platform that integrates both aerial and ground

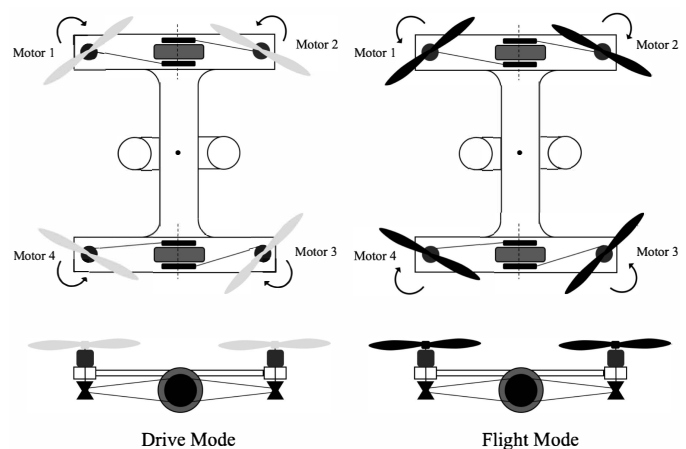


Fig. 3. Motor directions for drive and flight modes. In the flight mode, the propellers are engaged with the one-way bearings that allow torques to be transmitted to generate thrust. In the drive mode, the motors reverse and decouple the propellers. The motor speed differences are manipulated to provide full bidirectional ground mobility through the differentials.

mobility into a single compact vehicle. The design is organized into two distinct parts: the aerial side (top view) and the ground side (bottom view) as shown in Fig. 2.

The top side of the vehicle closely resembles a conventional quadcopter. It has four A2212 1400KV brushless motors mounted symmetrically on a 3D-printed PLA frame. Each motor drives an 8-inch double-blade (8045-2) propeller that has a one-way bearing press-fitted and glued into its mounting hole. A shaft collar is installed on the top of each motor shaft to constrain the propeller. In flight mode, the motors spin forward, and the one-way bearings lock and drive the propellers to generate thrust. For each propeller-motor pair, it can generate maximum 5.92N thrust with 3-cell battery. When the motors reverse for ground operation, the bearings allow the propellers to freewheel, effectively disengaging them so that energy is not wasted through propeller drag.

The bottom side of the vehicle houses the ground drivetrain. For ground propulsion, each pair of opposing motors transmits torque via small pulleys attached to extended shafts. These pulleys drive belts that connect to larger pulleys on the input

TABLE I
VEHICLE WEIGHT BREAKDOWN
(COMPONENTS FOR GROUND LOCOMOTION ARE LISTED ON THE RIGHT)

Components	Mass (g)	Ground Components	Mass (g)
Frame	201.2	Pulleys	9.5
Motors & Propellers	224.4	Belts	5.0
Electronics & Wires	82.2	Ball Casters	40.2
Battery	155.1	One-way Bearings	2.4
Ground Components	152.6	Wheels & Differentials	95.5
Grand Total	815.5	Ground Sub-total	152.6

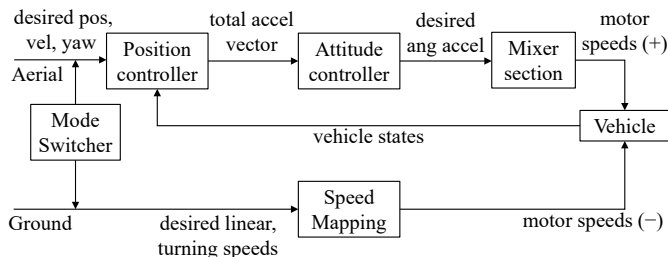


Fig. 4. The diagram of the two-mode control framework. In aerial mode, a closed-loop cascaded controller manages acceleration, with inputs coming from either manual controls (for outdoor flights) or an outer-loop position controller (for indoor MoCap flight). In ground mode, desired linear and rotational speeds are directly mapped to motor speed commands using factors such as gear ratio and wheel radius.

shafts of miniature differentials. Each differential then drives an integrated ground-contact wheel directly. The differential mechanism converts the relative speeds of the paired motors into bidirectional wheel rotation, enabling the vehicle to move forward, reverse, or execute turning maneuvers without additional actuators. To provide ground stability, two universal ball casters are mounted at the front and rear of the chassis via a thermoplastic polyurethane (TPU) damper. The vehicle is able to handle terrains with minor irregularities such as concrete, asphalt and compacted soil surfaces. For more uneven surfaces, the vehicle can simply transition to flight.

Our integrated configuration allows a quick transition between flight and ground modes through software-controlled reversal of motor rotation. In forward rotation (flight mode), the propellers are engaged to generate thrust, while in reverse rotation (ground mode) the propellers freewheel and the drivetrain, comprising the pulleys, belts, and differentials, provides efficient and bidirectional ground traction without extra actuators. Table I shows the weight breakdown of the vehicle components. It shows that the entire vehicle weighs only 815 g. Meanwhile, the weight of additional components for ground locomotion is 152.6 g, which only takes 18.7% of the total weight.

III. CONTROL

The vehicle uses a mode-switched control framework as shown in Fig. 4, which allows the same four motors to power either the propellers for flight or the ground wheels for driving. Mechanically, the belt-driven differentials remain engaged at all times, but the propellers are decoupled by one-way bearings when motors spin in reverse.

TABLE II
VEHICLE CONTROLLER PARAMETERS

Symbol	Parameter	Value
ω_{nat}	Natural frequency	2 Hz
ζ	Damping ratio	1
τ_{att}	Attitude time constant	[0.2, 0.2, 0.5] s
τ_{ω}	Rates time constant	[0.05, 0.05, 0.2] s
l	Adjacent rotor spacing	0.22 m
k	Propeller thrust to torque constant	0.014 m

A. Flight Mode

In flight mode, the motors rotate forward and the one-way bearings allow the motor shafts to transmit torque to the propellers. Similar to many existing quadcopters [27], [28], we employ a model-based cascaded controller architecture for Duawlf in the flight mode. The controller enables autonomous tracking of desired position, velocity, and yaw. The controller can be decomposed into a position controller, an attitude controller, and a mixer section.

1) *Position Controller*: The position controller in the outermost control loop takes the desired position \mathbf{p}_{des} from the autonomous trajectory tracking stack. It calculates the current estimated position \mathbf{p}_{est} and velocity \mathbf{v}_{est} by extended Kalman filter (EKF) from the position measurement of the motion capture (MoCap) system. Using these inputs, it computes the desired acceleration \mathbf{a}_{des} , then produce the total acceleration $\mathbf{a}_{tot} = \mathbf{a}_{des} + \mathbf{g}$ needed to follow the trajectory.

$$\mathbf{a}_{des} = \omega_{nat}^2 (\mathbf{p}_{des} - \mathbf{p}_{est}) + 2\zeta\omega_{nat}(\mathbf{v}_{des} - \mathbf{v}_{est}) \quad (1)$$

2) *Attitude Controller*: The attitude controller commands the vehicle's thrust direction to align with the desired total acceleration \mathbf{a}_{tot} while applying the desired yaw ψ_{des} . The estimated attitude \mathbf{R}_{est} is computed by EKF from the raw attitude measurement of MoCap system. The estimated angular velocity $\boldsymbol{\omega}_{est}$ is computed by another EKF that is onboard the vehicle using the IMU measurements. The controller first normalizes the total acceleration vector to obtain the unit vector $\hat{\mathbf{a}}_{tot}$. The intermediate vector \mathbf{n}_f is the rotation axis that aligns the world z -axis unit vector $\hat{\mathbf{z}}$ with $\hat{\mathbf{a}}_{tot}$, and β_f is the corresponding rotation angle. The function $\mathcal{R}_{\mathcal{M}}(\cdot)$ converts this axis-angle representation to a rotation matrix \mathbf{R}_f that aligns thrust with the acceleration command. The yaw command is applied by post-multiplying \mathbf{R}_f with a rotation about the z -axis, yielding the desired orientation \mathbf{R}_{des} . The function $\mathcal{V}(\cdot)$ converts the orientation error $\mathbf{R}_{est}^T \mathbf{R}_{des}$ into a 3D rotation vector, which is element-wise divided \oslash by the attitude control gain vector $\boldsymbol{\tau}_{att}$ to obtain the desired angular velocity $\boldsymbol{\omega}_{des}$. The angular velocity error \mathbf{e}_{ω} is computed by subtracting the current angular velocity from $\boldsymbol{\omega}_{des}$. This error is then element-wise divided by the rate control gain vector $\boldsymbol{\tau}_{\omega}$ to produce the desired angular acceleration $\boldsymbol{\alpha}_{des}$.

$$\hat{\mathbf{a}}_{tot} = \frac{\mathbf{a}_{tot}}{\|\mathbf{a}_{tot}\|} \quad (2)$$

$$\mathbf{n}_f = \hat{\mathbf{z}} \times \hat{\mathbf{a}}_{tot}, \quad \beta_f = \arccos(\hat{\mathbf{a}}_{tot} \cdot \hat{\mathbf{z}}) \quad (3)$$

$$\mathbf{R}_f = \mathcal{R}_{\mathcal{M}}([\mathbf{n}_f / \|\mathbf{n}_f\|, \beta_f]) \quad (4)$$

$$\mathbf{R}_{des} = \mathbf{R}_f \begin{bmatrix} \cos \psi_{des} & -\sin \psi_{des} & 0 \\ \sin \psi_{des} & \cos \psi_{des} & 0 \\ 0 & 0 & 1 \end{bmatrix} \quad (5)$$

$$\boldsymbol{\omega}_{des} = \boldsymbol{\tau}_{att} \otimes \mathcal{V}(\mathbf{R}_{est}^T \mathbf{R}_{des}) \quad (6)$$

$$\mathbf{e}_\omega = \boldsymbol{\omega}_{des} - \boldsymbol{\omega}_{est} \quad (7)$$

$$\boldsymbol{\alpha}_{des} = \boldsymbol{\tau}_\omega \otimes \mathbf{e}_\omega \quad (8)$$

3) *Mixer Section*: Given the vehicle's geometry, mass, inertia, and motor constants, the mixer allocates the total thrust and body torques into individual rotor thrusts. The total thrust command f_{tot} is computed from the vehicle mass m and the norm of the desired total acceleration \mathbf{a}_{tot} . The body torque vector $\boldsymbol{\tau}$ is obtained from the desired angular acceleration $\boldsymbol{\alpha}_{des}$ using the inertia matrix \mathbf{J} .

The allocation matrix in maps the roll τ_x , pitch τ_y , yaw τ_z torques, and total thrust f_{tot} into individual rotor thrusts f_1 – f_4 . Here, l is the horizontal distance from the vehicle's center to each rotor, and k is the ratio of torque to thrust for a single propeller. The resulting thrust values are converted to motor speeds using the propeller's thrust curve and sent to the electronic speed controller (ESC) as DShot commands. Key controller parameters are summarized in Table II.

$$f_{tot} = m \|\mathbf{a}_{tot}\| \quad (9)$$

$$\boldsymbol{\tau} = \mathbf{J} \boldsymbol{\alpha}_{des} \quad (10)$$

$$\begin{bmatrix} f_1 \\ f_2 \\ f_3 \\ f_4 \end{bmatrix} = \frac{1}{4} \begin{bmatrix} -1/l & -1/l & -1/k & 1 \\ -1/l & 1/l & 1/k & 1 \\ 1/l & 1/l & -1/k & 1 \\ 1/l & -1/l & 1/k & 1 \end{bmatrix} \begin{bmatrix} \tau_x \\ \tau_y \\ \tau_z \\ f_{tot} \end{bmatrix} \quad (11)$$

B. Ground Mode

In ground mode, the UAV's desired forward linear speed v_f (m/s) and angular speed ω_z (rad/s) from user inputs are used to compute the individual wheel speeds. The vehicle's right and left wheel speeds, w_r and w_l respectively, are defined as:

$$w_r = k_1 (v_f + k_2 \omega_z), \quad w_l = k_1 (v_f - k_2 \omega_z) \quad (12)$$

where k_1 is the inverse of the wheel radius and k_2 is the lateral offset of the wheels from the vehicle center. Motor commands for ground mode are derived from the calculated wheel speeds. Let w_i denote the idle motor speed, and let $\omega_1, \omega_2, \omega_3$, and ω_4 represent the commanded motor speeds for the four motors in their reverse directions. These are computed as follows:

$$\begin{aligned} \omega_1 &= -k_3 w_r + w_i, & \omega_2 &= k_3 w_r + w_i, \\ \omega_3 &= k_3 w_l + w_i, & \omega_4 &= -k_3 w_l + w_i \end{aligned} \quad (13)$$

where w_r and w_l are the right and left wheel speeds defined in Equation (12), and k_3 is the reduction ratio of the pulley-belt transmission. For robust ground operation, the motors are maintained above the nominal idle speed, and the minimum commanded speed is defined as

$$\omega_{\min} = w_i \quad (14)$$

If any computed motor command ω_i falls below ω_{\min} , that command is raised to ω_{\min} and the paired motor's command is

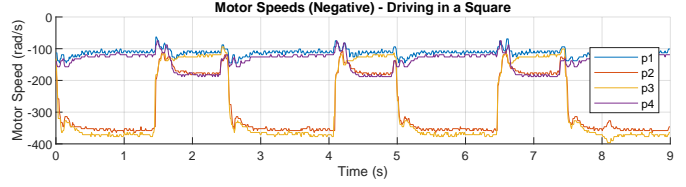
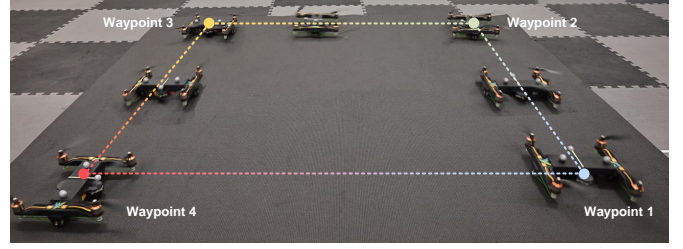


Fig. 5. Motor speed profiles for a complete square-path maneuver in the ground mode. The vehicle departs waypoint 1 and reaches waypoint 2 at $t = 1.5$ s, then performs a 90° in-place rotation from $t = 1.5$ s to 2.5 s. It travels to waypoint 3, arriving at $t = 4.0$ s, executes a second 90° turn from $t = 4.0$ s to 5.0 s, then moves to waypoint 4, arriving at $t = 6.5$ s. At waypoint 4 it performs a third 90° rotation between $t = 6.5$ s and 7.5 s before returning toward waypoint 1 to complete the square.

increased by the same amount to maintain the required speed differential. For example, if for a pair of motors the computed commands are ω_1 and ω_2 and $\omega_1 < \omega_{\min}$, then the adjustments are performed as follows:

$$\omega_1 \leftarrow \omega_{\min} \quad \text{and} \quad \omega_2 \leftarrow \omega_2 + (\omega_{\min} - \omega_1) \quad (15)$$

This ensures that the intended speed difference $\omega_2 - \omega_1$ is maintained while avoiding operation in the low-performance startup region of sensorless brushless motors. These final motor commands are then sent to the ESC as DShot signals, using an open-loop mapping calibrated from wheel speed tests.

To illustrate ground-mode behavior, we plot motor speeds for a simple square-path driving test. As shown in Fig. 5, when the vehicle is moving in a straight line between every two waypoints, the rear motors on each side spin faster than the front motors, which remain at the minimum speed ω_i : $|\omega_2| > |\omega_1| = |\omega_i|$ and $|\omega_3| > |\omega_4| = |\omega_i|$, causing both wheels to move forward. When the vehicle is turning around itself at a waypoint, the speed relationship becomes $|\omega_2| > |\omega_1| = |\omega_i|$ and $|\omega_4| > |\omega_3| = |\omega_i|$, so the right wheel continues to advance while the left wheel reverses, making the vehicle turn counterclockwise.

Mode switching does not require any physical reconfiguration beyond reversing motor spin directions. The high-level autonomy stack (or a user command) selects flight or drive mode, causing the controller to generate motor speed setpoints for either aerial thrust (forward rotation) or ground travel (reverse rotation). This unified approach enables rapid transitions with low mechanical complexity while preserving the vehicle's standard quadrotor functionality in flight.

IV. EXPERIMENTAL VALIDATION

The proposed hybrid UAV was evaluated in four sets of experiments that test its performance in both flight and ground modes, as well as its ability to transition seamlessly between

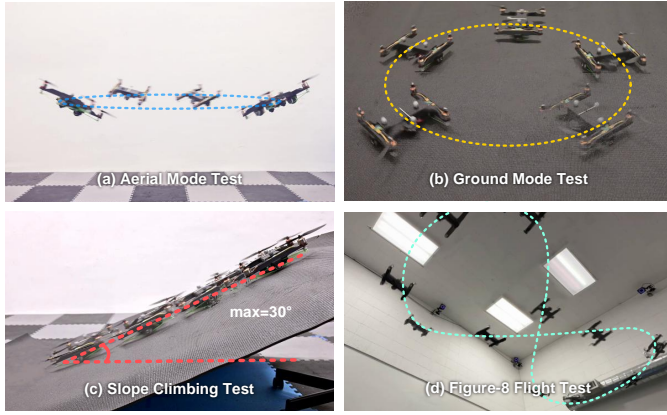


Fig. 6. Time-lapse pictures of experiments. To test the power consumption and lateral acceleration under two different modes, we test and record the data when (a) Duawlfm flying in a circle. (b) Duawlfm driving in a circle. To explore the maximum slope-climbing capability, we let (c) Duawlfm drives up a ramp up to 30° . To test the performance of proposed controller, we make (d) Duawlfm fly along the figure-8 trajectory.

these modes. Below, we present the key experiments along with discussions that highlight the performance trade-offs, advantages, and implications of the design. All power and energy consumption data are computed from current and voltage measurements obtained by the onboard sensors. All position measurements are recorded using the MoCap system. Motor speed measurements are obtained from the onboard BLHeli32 ESC readings.

A. Circular Motion Experiment

TABLE III
AVERAGE POWER CONSUMPTION DURING CIRCULAR MOTION (1-METER DIAMETER) AT VARIOUS SPEEDS IN FLIGHT AND GROUND MODES

Speed (m/s)	Lateral G-force (g)	Fly Power (W)	Drive Power (W)
1.0	0.20	124.6	3.9
1.5	0.46	140.6	8.2
2.0	0.82	188.8	14.9

To evaluate maneuverability and efficiency during tight turning motions, circular paths with a radius of 1 meter were tested in both flight and ground modes at speeds ranging from 1.0 to 2.0 m/s. Fig. 6.(a) and (b) show the experiment footage. Table III summarizes the average power consumption for 5 seconds and the lateral acceleration experienced in each scenario. We test the power consumption of our vehicle with a 3-cell 2200 mAh battery. For reference, the maximum hovering time of our vehicle is 10.5 min under this configuration.

The results clearly demonstrate that for rapid turning maneuvers, the ground mode significantly outperforms flight mode in terms of energy-efficiency. At 1.0 m/s, ground-mode operation consumes only 3.9 W, whereas flight mode requires 124.6 W, which is over 30 times higher. Even at increased speeds of up to 2.0 m/s, ground mode maintains drastically lower power demands compared to flight mode (14.9 W versus 188.8 W). This substantial difference arises because vehicle is not required to carry the weight and overcome the gravity.

Additionally, ground-mode operation exhibits high agility, which can comfortably handle maneuvers with 0.82 g lateral accelerations at 2.0 m/s. This indicates that the hybrid vehicle is not only energy-efficient but also highly capable of rapid directional changes in confined spaces, making it especially suitable for dynamic urban and indoor environments where tight maneuvering is frequently required.

In summary, the data confirms that ground-mode operation provides a marked advantage in energy-efficiency and agility for short-range, rapid-turning maneuvers, enhancing the overall practicality and versatility of the hybrid UAV in realistic deployment scenarios.

B. Slope Climbing Ability

TABLE IV
MEASURED ENERGY CONSUMPTION PER UNIT HEIGHT CLIMBED ON DIFFERENT SLOPE ANGLES

Slope Angle ($^\circ$)	Mean Power (W)	Energy / Height (J/m)
5	4.0	50.9
10	4.6	37.9
15	4.5	27.5
20	4.5	24.8
25	5.0	25.9
30	5.4	26.5

To assess the ground-mode capability of the Duawlfm, climbing experiments as shown in Fig. 6(c) were conducted with slope inclines ranging from 5° to 30° at a fixed forward speed of 0.5 m/s. The average power consumption and energy expenditure per unit height climbed were measured and summarized in Table IV.

The experimental results highlight several important aspects of Duawlfm's ground performance. First, the power requirements for slope climbing remain consistently low, averaging between 4.0 W to 5.4 W across all tested angles, demonstrating high drivetrain efficiency. The data indicate that climbing is inherently energy-efficient, particularly on steeper slopes where the energy required per unit height actually decreases due to reduced traversal distance, reaching as low as 24.8 J/m at 20° . This trend shows the system's effectiveness at converting energy into vertical displacement.

Additionally, the vehicle demonstrates robust climbing capabilities, successfully managing steep inclines up to 30° , at which point tire slippage begins to occur. Notably, a 30° incline already represents a significantly challenging gradient far exceeding typical accessibility ramps mandated by ADA standards (maximum 4.76°). Thus, the UAV's climbing performance comfortably surpasses real-world urban navigation requirements, including indoor environments and common building terrains. These findings confirm that the differential drivetrain provides consistent, efficient, and reliable performance even on steep slopes, making the UAV highly suitable for versatile deployment scenarios involving varied terrain conditions.

C. Figure-8 Flight Test

The addition of one-way bearings and an integrated ground drivetrain alters Duawlfm's rotor dynamics compared to a

TABLE V
HOVER AND FIGURE-8 FLIGHT PERFORMANCE

Vehicle	Hover Power (W)	Fig.-8 RMSE (cm)	Fig.8 Power (W)
Baseline	120.57	10.93	134.19
Duawlfm	124.35	9.74	138.53

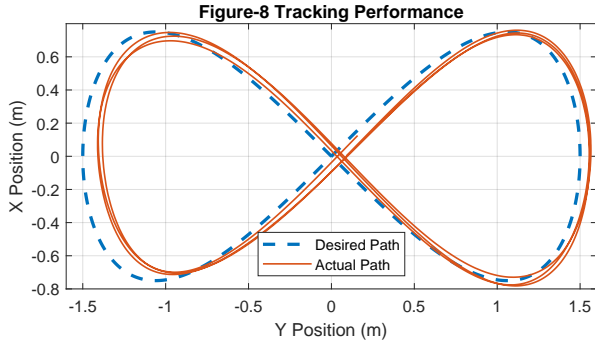


Fig. 7. Figure-8 flight test: the actual path (solid) of Duawlfm closely follows the desired trajectory (dashed), despite the additional inertial load of the ground drivetrain.

conventional quadcopter. Because the one-way bearings block reverse torque transmission, active propeller braking is no longer possible. Moreover, the ground drivetrain remains engaged even in flight, so each rotor must accelerate the pulleys, belt, and differential, adding inertia and introducing frictional losses. We argue that, despite these extra loads, the effects on performance are minimal. Propeller drag alone suffices to slow the rotors at an acceptable rate in the absence of active braking, as is common in many drones where the ESC does not employ active braking. Additionally, the drivetrain components, such as plastic pulleys, are lightweight, resulting in only a small increase in total rotor inertia.

To investigate these effects, we executed a 3-cycle figure-8 trajectory tracking flight on Duawlfm and a baseline vehicle. The figure-8 trajectory is of 1.5 m major diameter with the vehicle flying at a speed of 2 m/s as shown in Fig. 6(d). The baseline vehicle is a modified Duawlfm with the same propellers but without the one-way bearings and with its ground drivetrain disconnected; all other parameters remain identical. Fig. 7 overlays the desired (dashed) and actual (solid) flight paths of Duawlfm, and Table V summarizes the quantitative results of Duawlfm and the baseline vehicle in both hover flights and figure-8 trajectory tracking.

The data indicate that Duawlfm’s trajectory tracking root-mean-squared error (RMSE) is small and comparable to the baseline, demonstrating that the added drivetrain components have virtually no effect on tracking performance. Both hover power and figure-8 trajectory tracking power are only about 3.23% higher than those of the baseline, so the ground drivetrain imposes only a minor penalty on energy-efficiency due to friction losses. These results confirm that the design modifications preserve robust aerial performance suitable for real-world UAV applications.

In theory, active propeller braking and complete drivetrain disengagement in flight could still be implemented. Examples

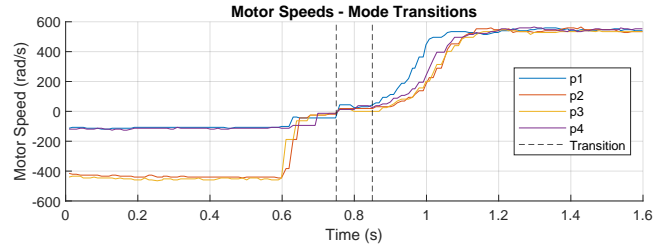
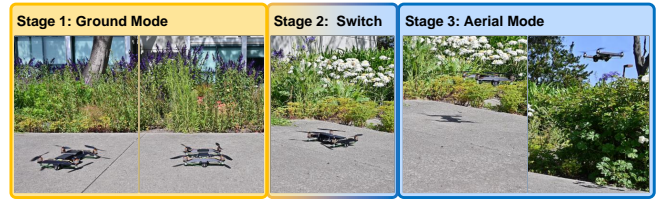


Fig. 8. The demonstration of outdoor multi-terrain test. Stage 1: Duawlfm is running on the sidewalk. Stage 2: Duawlfm switches from its ground mode into aerial mode. The mode switch is completed in 0.1s Stage 3: Duawlfm takes off and flies over the bush. With the complex terrain where the wheel locomotion cannot handle, the motors actuate propellers directly and enables the robot fly over it.

include either actively with servos or passively with clutches that engage when thrust is applied. However, the results presented here represent the most conservative case (drivetrain always engaged and no active braking), and even under these conditions the vehicle performs well.

D. Outdoor Multi-Terrain Test

We performed a multi-terrain demonstration to showcase Duawlfm’s ability to transition between air and ground modes in a simulated delivery scenario. Specifically, we simulated a package delivery task from one building to another. For brevity and analytical clarity, only the initial phase, which is taking off and transitioning from ground to air outside the origin building, is presented here. Unlike all the other experiments, the flight mode controller in this part does not involve the position controller, and the vehicle is controlled manually with joystick-controlled acceleration instead. Fig. 8 presents the results, with the top panel showing a time-lapse of the vehicle’s path as it takes off from ground mode and transitions into flying, and the bottom panel displaying motor speeds and power consumption over time.

The vehicle data plot illustrates how quickly the vehicle can switch the operational mode by having the motors switch direction, from negative (driving the wheels) to positive (generating lift), with a very short delay. This quick reversal of motor direction confirms that Duawlfm’s transition mechanism is both mechanically simple and dynamically responsive, enabling efficient deployment for delivery tasks requiring frequent mode changes. Overall, this demonstration highlights the UAV’s practical suitability for real-world urban logistics, showcasing its fast, stable, and energy-efficient transitions between aerial and ground operation modes.

V. CONCLUSION

We introduced Duawlfm, a drone with unified actuation for wheeled locomotion and flight operation that achieves

efficient, bidirectional ground mobility without requiring additional actuators or relying on propeller thrust for terrestrial propulsion. The design employs one-way bearings and a differential system to repurpose existing quadrotor motors for both aerial flight and ground driving. This streamlined approach significantly reduces mechanical complexity, system weight, and energy usage while ensuring robust multimodal functionality. Experimental validation confirmed the effectiveness and practicality of our hybrid robot across various scenarios. Flight tests indicated minimal performance trade-offs, with only minor increases in energy consumption compared to a conventional quadrotor in the flight mode. Ground-mode experiments demonstrated impressive efficiency, successfully navigating steep slopes of up to 30° and performing agile turns with lateral accelerations close to $1g$, all while using significantly less energy than flying. The multi-terrain demo showcased the robot's smooth and rapid transitions between aerial and terrestrial modes, underscoring its real-world applicability for urban delivery and indoor navigation tasks.

ACKNOWLEDGMENT

This work was supported by Hong Kong Center for Logistics Robotics. The experimental testbed at the HiPeRLab is the result of the contributions of many people, a full list of which can be found at <https://hiperlab.berkeley.edu/members/>.

REFERENCES

- [1] M. W. Mueller, S. J. Lee, and R. D'Andrea, "Design and control of drones," *Annual Review of Control, Robotics, and Autonomous Systems*, vol. 5, no. 1, pp. 161–177, 2022.
- [2] R. Thusoo, S. Jain, and S. Bangia, "Quadrotors in the present era: a review," *Information Technology in Industry*, vol. 9, no. 1, pp. 164–178, 2021.
- [3] F. Samouh, V. Gluza, S. Djavadian, S. Meshkani, and B. Farooq, "Multimodal autonomous last-mile delivery system design and application," in *2020 IEEE International Smart Cities Conference (ISC2)*, pp. 1–7, IEEE, 2020.
- [4] A. M. Raiivi, S. A. Huda, M. M. Alam, and S. Moh, "Drone routing for drone-based delivery systems: A review of trajectory planning, charging, and security," *Sensors*, vol. 23, no. 3, p. 1463, 2023.
- [5] R. Bridgellall, T. Askarzadeh, D. Tolliver, M.-P. Consortium, *et al.*, "Remote sensing of multimodal transportation assets using drones," tech. rep., Mountain-Plains Consortium, 2024.
- [6] K. P. Jain, J. Tang, K. Sreenath, and M. W. Mueller, "Staging energy sources to extend flight time of a multirotor uav," in *2020 IEEE/RSJ International Conference on Intelligent Robots and Systems (IROS)*, pp. 1132–1139, 2020.
- [7] A. Kalantari, T. Touma, L. Kim, R. Jitosh, K. Strickland, B. T. Lopez, and A.-A. Agha-Mohammadi, "Drivocopter: A concept hybrid aerial/ground vehicle for long-endurance mobility," in *Proceedings of the 2020 IEEE Aerospace Conference*, pp. 1–10, 2020.
- [8] Y. Qin, Y. Li, X. Wei, and F. Zhang, "Hybrid aerial-ground locomotion with a single passive wheel," in *2020 IEEE/RSJ International Conference on Intelligent Robots and Systems (IROS)*, pp. 1371–1376, 2020.
- [9] K. Sugihara, M. Zhao, T. Nishio, K. Okada, and M. Inaba, "Design and control of delta: Deformable multilinked multirotor with rolling locomotion ability in terrestrial domain," *arXiv preprint arXiv:2403.06636*, 2024.
- [10] J. R. Page and P. E. I. Pounds, "The quadroller: Modeling of a uav/ugv hybrid quadrotor," in *2014 IEEE/RSJ International Conference on Intelligent Robots and Systems*, pp. 4834–4841, 2014.
- [11] H. Jia, R. Ding, K. Dong, S. Bai, and P. Chirarattananon, "Quadrollor: A reconfigurable quadrotor with controlled rolling and turning," *IEEE Robotics and Automation Letters*, vol. PP, pp. 1–8, 07 2023.
- [12] S. Sabet, A.-A. Agha-Mohammadi, A. Tagliabue, D. S. Elliott, and P. E. Nikravesh, "Rollocopter: An energy-aware hybrid aerial-ground mobility for extreme terrains," in *2019 IEEE Aerospace Conference*, pp. 1–8, 2019.
- [13] C. Premachandra, M. Otsuka, R. Gohara, T. Ninomiya, and K. Kato, "A study on development of a hybrid aerial / terrestrial robot system for avoiding ground obstacles by flight," *IEEE/CAA Journal of Automatica Sinica*, vol. 6, no. 1, pp. 327–336, 2019.
- [14] S. Bai, Q. Pan, R. Ding, H. Jia, Z. Yang, and P. Chirarattananon, "An agile monopodal hopping quadcopter with synergistic hybrid locomotion," *Science robotics*, vol. 9, p. eadi8912, 04 2024.
- [15] N. Pan, J. Jiang, R. Zhang, C. Xu, and F. Gao, "Skywalker: A compact and agile air-ground omnidirectional vehicle," *IEEE Robotics and Automation Letters*, vol. 8, no. 5, pp. 2534–2541, 2023.
- [16] R. Zhang, J. Lin, Y. Wu, Y. Gao, C. Wang, C. Xu, Y. Cao, and F. Gao, "Model-based planning and control for terrestrial-aerial bimodal vehicles with passive wheels," in *2023 IEEE/RSJ International Conference on Intelligent Robots and Systems (IROS)*, pp. 1070–1077, 2023.
- [17] J. Lin, R. Zhang, N. Pan, C. Xu, and F. Gao, "Skater: A novel bi-modal bi-copter robot for adaptive locomotion in air and diverse terrain," *IEEE Robotics and Automation Letters*, vol. 9, no. 7, pp. 6392–6399, 2024.
- [18] S. Yu, B. Pu, K. Dong, S. Bai, and P. Chirarattananon, "A hybrid quadrotor with a passively reconfigurable wheeled leg capable of robust terrestrial maneuvers," *IEEE Robotics and Automation Letters*, vol. PP, pp. 1–8, 01 2025.
- [19] F. Saemi, A. Whitson, and M. Benedict, "Heat transfer models and measurements of brushless dc motors for small uavs," *Aerospace*, vol. 11, no. 5, p. 401, 2024.
- [20] S. Morton and N. Papanikolopoulos, "A small hybrid ground-air vehicle concept," in *2017 IEEE/RSJ International Conference on Intelligent Robots and Systems (IROS)*, pp. 5149–5154, 2017.
- [21] M. Zhao, T. Anzai, and T. Nishio, "Design, modeling, and control of a quadruped robot spider: Spherically vectorable and distributed rotors assisted air-ground quadruped robot," *IEEE Robotics and Automation Letters*, vol. 8, no. 7, pp. 3923–3930, 2023.
- [22] K. Sugihara, M. Zhao, T. Nishio, T. Makabe, K. Okada, and M. Inaba, "Design and control of a small humanoid equipped with flight unit and wheels for multimodal locomotion," *IEEE Robotics and Automation Letters*, vol. 8, no. 9, pp. 5608–5615, 2023.
- [23] K. Kim, P. Spieler, E. S. Lupu, A. Ramezani, and S.-J. Chung, "A bipedal walking robot that can fly, slackline, and skateboard," *Science Robotics*, vol. 6, p. Art. No. eabf8136, Oct 2021. Funding by Caltech Gary Clinard Innovation Fund.
- [24] A. R. S. and m. m. Dharmana, "Multi-terrain multi-utility robot," *Procedia Computer Science*, vol. 133, pp. 651–659, 01 2018.
- [25] E. Sihite, A. Kalantari, R. Nemovi, A. Ramezani, and M. Gharib, "Multi-modal mobility morphobot (m4) with appendage repurposing for locomotion plasticity enhancement," *Nature communications*, vol. 14, no. 1, p. 3323, 2023.
- [26] W. D. Shin, H.-V. Phan, M. A. Daley, A. J. Ijspeert, and D. Floreano, "Fast ground-to-air transition with avian-inspired multifunctional legs," *Nature*, vol. 636, no. 8041, pp. 86–91, 2024.
- [27] M. W. Mueller, "Multicopter attitude control for recovery from large disturbances," *arXiv preprint arXiv:1802.09143*, 2018.
- [28] M. W. Mueller, *Dynamics and Control of Autonomous Flight*. Springer Nature, 2025.